# Embryo timelapses can be compiled and quantified to understand canonical histone dynamics across multiple cell cycles.

**Lydia Smith[1] and Paul Maddox[2]**

[1]Department of Genetics and Molecular Biology, University of North Carolina at Chapel Hill, NC, 27599
[2]Department of Biology, University of North Carolina at Chapel Hill, NC, 27599

Address correspondence to: Paul S. Maddox at pmaddox@email.unc.edu

**Abstract**

In the last decade, computational analysis of big datasets has facilitated the processing of unprecedented quantities of collected biological data. Thus, automations and big data analyses have been revolutionary in detecting and quantifying subtle phenotypes in cell biological contexts. Analyzing similar quantities of data in larger and more complicated biological systems such as live embryos has been more challenging due to experimental necessities impeding both compilations of data collection and informative analysis. Here we present a streamlined workflow that can quantify cell cycle dynamics in early developing embryos using fluorescently labeled proteins. We benchmark this pipeline using *Caenorhabditis elegans* (nematode) embryonic development and a fluorescently labeled histone. Using our pipeline, we find that histone proteins are broadly stable in early embryonic development. In sum, we have utilized the large biological and experimental variation associated with quantification of fluorescent proteins in embryonic systems, to quantify nuclear accumulation rate, chromatin incorporation, and turnover/stability of canonical histones during early development.

## Introduction

The ability to measure the quantities and dynamics of chromatin organizing proteins throughout progressive cell cycles has been widely used for decades. Conventional quantification of cell cycle components using either yeast or mammalian cultured cells have taken advantage of the ability to synchronize a culture of hundreds or thousands of cells making it possible to perform western blots from cells all at nearly perfectly analogous stages within the cell cycle[1][2]. More recently, high resolution and magnification (NA >1, 60x+ magnification) fluorescence microscopy has been utilized as an alternative method of quantifying levels of fluorescently labeled proteins during the cell cycle. One of the advantages of fluorescence microscopy is it allows for the quantification of proteins in live cells, using either fluorescently labeled proteins or active dyes, facilitating protein quantification at the single cell level. Mammalian cell cultures and yeast have been the workhorses of *in vivo* quantitative fluorescent microscopy, due to the plethora of molecular tools available enabling fluorescent tagging of proteins, insertion of expression vectors, and the introduction of active dyes into cells. They are also ideal for imaging as they have little movement in 3D and have relatively thin vertical profiles, resulting in fluorescent proteins being in close proximity of the coverslip, resulting in a high signal to noise ratio[3][4]. And their immortal, synchronous, and symmetric cell cycles make statistical analysis of the data easy to perform; much of which now can be automated [5][6].

In order to measure histone dynamics in embryos, accurate cell cycle quantifications are required. In contrast to the live-imaging of eukaryotic cell cultures, there are several challenges involved in trying to quantify fluorescent proteins in the developing tissues of embryos. These include non-uniform cell architecture (variable sizes and shapes), typically short, rapid cell cycles (followed by increasingly lengthening cell cycles[7]), an inability to pause or synchronize cell cycles (due to weak cell cycle checkpoints[8] or impermeable eggshells[9]), and significant movement of cells/nuclei throughout development[10].

First developed as a model system by Sydney Brenner, the soil-dwelling, non-parasitic nematode *C. elegans* embryo has been a workhorse for embryology studies for the past 50 years because of its transparent egg shell and invariant development[11][12]. In addition, *C. elegans* was the first organism to be utilized to express the revolutionary fluorescent protein GFP[13]. This precipitated the eventual incorporation of automated tracking of fluorescent proteins throughout development[14], as has been utilized for other cultured systems, although quantifying the

fluorescent proteins they track in these systems has lagged. Like many other embryonic systems used in the laboratory[15], *C. elegans* embryos have several physical characteristics that make quantification of fluorescence microscopy experiments challenging to perform. First, whereas the phases of mitosis are easy to temporally distinguish do to the condensation and behavior of chromosomes, *C. elegans* embryos lack conventional gap phases, resulting in unique events between mitoses difficult to temporally distinguish. Second, it is virtually impossible to collect synchronized populations of cells/embryos, precluding bulk biochemical and/or immunofluorescence analyses. Third, *C. elegans* embryos are ~20-25µm in diameter (in the shortest dimension, ~50um in the long axis), resulting in a large enough volume for cells/nuclei to migrate, either passively through progressive cell cycles, or actively through tissue migration events like gastrulation[12][16][17]. This results in exponentially decreasing collection of fluorescence signal from individual cells/nuclei throughout the embryo when using the required high NA optics (NA>1.0) [18].

All of this results in data that is much more variable than can be collected from cultured cell data. When using quantification of image data-sets generated using light microscopy to measure protein levels, there are inherently two large sources of variation within the data: biological and experimental. Although there are ways to minimize the amount of biological variability by maintaining consistent imaging and culturing conditions[12], it is impossible to eliminate true biological variation. Therefore, we focused our analysis efforts on eliminating experimental variation in our analysis in order to create a model of protein dynamics in an "average embryo". In cell culture, where a relatively homogenous group of cells can be synchronized, it is possible to easily average quantifiable information about the cells at specific parts of the cell cycle. It is also possible to sort non-synchronized cells either through similarity in cell cycle progression (every cell progresses through the cell cycle identically allowing post-acquisition alignment of data[19]) or bulk snap shot analysis. Here we have exploited the stereotypical development in *C. elegans* to create an analysis pipeline to quantify histone dynamics through post-acquisition alignment of data. The *C. elegans* system facilitates the comparison of multiple differentiated lineages from as early as the 2-cell stage until hatching and has made it possible to analyze embryogenesis using either differential interference contrast (DIC) microscopy or fluorescently labeled proteins[14]. This ease of visibility of all of the cells of the developing embryo has been instrumental in developing our understanding of the spatial and temporal regulation of a plethora of proteins, transcripts, and developmental factors.

To perform post-acquisition alignment of data, we took advantage of *C. elegans'* stereotypical development by utilizing embryonic equivalence. We define embryonic equivalence as the assumption that in highly stereotypical embryogenesis such as *C. elegans*[11][14], developmentally identical cells between embryos will have equivalent biological measurables; this includes cell cycle length, size, position, protein levels, etc. This embryonic equivalence allows us to average quantifications from multiple embryos in order to reduce experimental variability and build a model of an average embryo. As long as all the timelines share at least one common cellular event, all time-lapses can be both normalized and organized temporally together. Because the length of the cell cycles fluctuates a small amount based on environmental and imaging conditions, we aligned the timelapses to the last time point of a cell's lifespan. In our case, this was determined by the last timepoint when the mitotic chromatin was still one mass, and not divided into two groups during anaphase (Figure 1A). This approach has allowed us to quantify histones in early development and could easily be transformed to other cellular components (e.g. microtubules, Golgi, ER, etc.) in *C. elegans* or other complex cellular systems such as embryos or organoids.

## Results

### Embryonic time-lapse data can be organized like cell culture data to create a model of an "average" embryo.

To quantify the dynamics and quantities of histones in developing embryos, we utilized a strain of *C. elegans* that has one copy of H2B (*his-58*) tagged with mCherry. Each cell cycle, the amount of H2B in each nucleus or incorporated into chromatin is measured over time by fluorescence intensity. We focused primarily on three early lineages; two somatic lineages, AB and E, as well as the germline lineage P (Figure 1A). Embryos were imaged within 3D stacks with 2-minute intervals for 1-3 hours. Given that later in the pipeline timelapses will be reconstructed and reorganized, multiple non-synchronized embryos can be imaged simultaneously to maximize data gathered per image (Figure 1B). Each nucleus of the appropriate lineages from every embryo is quantified, background and bleach corrected (Equations 1-2) and given a timestamp.

$$BleachCorrected\ RID\ (Nuclear_{ROI}(t)) = RID(Nuclear_{ROI}(t)) * (\frac{ave{:}MGV(1-3)}{ave{:}MGV(t)}) \quad (1)$$

$$Background\&BleachCorrected\ RID\ (Nuclear_{ROI}(t)) = BleachCorrected\ RID\ \left(Nuclear_{ROI}(t)\right) - (ave{:}\ BleachCorrected\ RID\ \left(Background_{ROI}(t)\right) * (\frac{area{:}Nuclear_{ROI}}{area{:}Background_{ROI}}) \quad (2)$$

For our primary analysis, all timestamps are aligned to the last time-point before each cell's anaphase (i.e. approximately metaphase) with the last image being set to 0. Time-lapse values can also be normalized further on a lineage specific basis. When normalized on a lineage by lineage basis, the values at a shared cellular event are set to 1, and all other values in that lineage are normalized accordingly (Figure 1C). From either of these analyses an average value can be generated at each time-point to build a profile of the relative quantities of a histone throughout cell cycles and lineages. Experimental data from the germline P-lineage (Figure 1D) and the somatic E- and AB- lineages (Figure 1E) are shown.

In order to image the embryos for long periods without significantly bleaching or inducing phototoxicity within the embryos, we took stacks of images through the embryos every two minutes. To overcome temporal under-sampling of the data, we developed a MATLAB macro that automatically explores all the possible combinations of aligning the timelapses in an attempt to decrease the overall standard deviation around the average we had previously generated. This macro allows us to interleave the timelapses by fitting similarly shaped curves closer mathematically[20](Boudreau et al 2018, in prep). All the timelapses maintain their normalized values, and time-points are maintained at 2 minutes apart. However, the timelapses of each cell cycle are shifted within a 4-minute (±2 minutes) interval by the algorithm either forward (>, >>) or backwards (<, <<) in time (Figure 1F). Actual experimental data for the P-lineage are shown in Figure 1G, and somatic E- and AB-lineages in Figure 1H.

To determine the dynamics of H2B in each cell cycle, we compared the relative last timepoint values of H2B signal derived from our "average embryo" pipeline (Figure 2B). To calculate the rate of histone nuclear accumulation during all of the observed cell cycles, we quantified the duration of each cell cycle wherein the nuclear signal rose in minutes (Table 1 Columns 1-2). We then normalized all of the timelapses to the relative value at each lineage's representative at the 4-cell stage (Table 1 Column 3). This number was multiplied by the amount

of histone to be added during DNA replication and then divided by the import duration to calculate nuclear accumulation (Table 1 Columns 4-5 and Equation 3).

$$(9.9 \cdot 10^5 * \frac{Metaphase\ Level(n)}{Metaphase\ Level(4-cell\ stage)})/Import\ Duration(n) \quad (3)$$

For this calculation we made the assumption that the histones roughly double every cell cycle and that there are roughly 1 million H2B histones added each cell cycle. This is based on *C. elegans'* 100Mb diploid genome size[21] divided by 147bp wrapped around each histone with an average 50bp[22] DNA linker with 2 H2B histones per nucleosome. Interestingly, we found an exponential decrease of nuclear accumulation rates as cell cycle length increases; a 6.7 min decrease half-life of accumulation for our H2B nuclear accumulation curve indicating that with every 6.7-minute increase to a cell cycle's length, there is a halving of the rate of nuclear accumulation.

**_C. elegans_ canonical histones are stability incorporated during early embryogenesis.**

Given that gross behaviors of histones relative to mitosis were not different between early developmental states (lineages), we turned to a different fluorescent assay, Fluorescence Redistribution After Photobleaching (FRAP). Utilizing the same strain of *C. elegans* as mentioned above, we focused our efforts on measuring the turnover of histones from the beginning to end of each cell cycle in early embryos. The most common method of measuring protein stability and turnover rates, FRAP involves photobleaching all of the fluorophores in a particular region of interest and quantifying both the quantity and rate of recovered fluorescent signal in that area. Typically, these types of experiments involve an internal non-bleached control. In our case, we wanted to bleach the entire pool of fluorophores in the nucleus, meaning that there would be no corresponding non-bleached homologous region to compare it to. Instead of traditional controls, we used the nuclear signal of non-bleached embryos as our control (Figure 3A).

To determine H2B dynamic incorporation into the nucleus, the amount of fluorescent signal in the nucleus was measured over the cell cycle in bleached and unbleached samples. In order to calculate the fraction of recovered signal, we normalized all of the timelapses to their first time-point (no bleach correcting) and calculated the increase in the controls (Figure 3B-C and Equation 4), then subtracted that average increase from each of our recovery FRAP signal

turnover (Figure 3D).

$$Turnover(n) = Background\&BleachCorrected\ Final\ FRAP(n) - (ave{:}\ Background\&BleachCorrected\ Final\ Controls) - 1) \quad (4)$$

This final value was calculated along with our FRAP efficiently which was around 70% (meaning on average 70% of the measured signal disappeared post-laser ablation with about 30% remaining). We find that all of the cells of the early embryo examined fall within the experimental error margins around 0%. We also find that this relationship really does not change when we separate the cells based on cell cycle length/developmental stage instead of cell cycle (Figure 3E). From the FRAP curves, we can also calculate the rate at which the signal recovers in each cell cycle[23] (Figure 3F) as well as the inverse of how long it takes each cell to recover their signal (Figure 3F and Equations 5-6).

$$\mathrm{t}_{1/2} = \mathrm{abs}\left|\mathrm{slope}\left(\frac{\mathrm{time}(min)|\ \mathrm{t}_1\mathrm{t}_2\mathrm{t}_{3\ldots}\mathrm{t}_\mathrm{n}}{\mathrm{signal(AU)}|\ \ln_1^\mathrm{n}(\mathrm{MaxRID}-\mathrm{RID(t)})}\right)\right| \quad (5)$$

$$\mathrm{RecoveryRate} = \frac{ln(2)}{\mathrm{t}_{1/2}} \quad (6)$$

For either measurement, there is not a strong correlation between cell type (soma/germ), cell cycle length, or developmental stage and the very slow rate at which the cells replenish their histones (Figure G-H).

## Discussion

Here we have used a quantitative microscopy analysis pipeline to investigate histone dynamics in early embryonic development. As genome activity changes, so does histone stability; transcriptionally silent regions have more histone stability[24][25]. In *C. elegans* embryos, transcription is activated in varying lineages at differing times [26], thus it could be possible to detect these changes by probing histone population dynamics. We have found that gross histone dynamics are canonical (follow that reported in other model systems) in *C. elegans* with very little variation in differing lineages. This result could indicate that genome regulation in early development leads to histone stabilization, or that these changes are highly focused and thus not

detected in our assays. Despite this, our work has derived a new imaging analysis pipeline and shows that histones in rapidly dividing embryonic cells follow expected behaviors.

One persistent complication to studying protein dynamics in embryos using light microscopy is the large amount of experimental variability that is added into any quantitative analysis attempted. Because the cells in a developing embryo are more demanding in their preferred environmental conditions than traditional cell cultures, creating an ideal quantitative environment has been a challenge for quantitative microscopists. In order to generate an 'average embryo', we found that normalizing, aligning, and averaging of many individual embryo timelapses is an effective way to understand the dynamics of cell cycle proteins throughout early embryo cell cycles. The resulting analyses can be differentially organized to answer specific biological questions. In our case, we were able to create models of 'average embryos' in early *C. elegans* embryos and describe the protein dynamics of individual cells/lineages. Utilizing our quantification and analysis pipeline, we focused our efforts on determining how H2B levels fluctuate throughout the cell cycles of developing lineages in the early embryo. We chose H2B as our initial protein to start with given that it is an incredibly well conserved protein across phylogeny[27] with well characterized cell cycle dynamics and characteristics[28].

Although our fluorescent histone is driven by a germline specific promoter (pie-1), it is unclear why such a strong and consistent amount of signal is present in all of the somatic cells[29]. We predict that it is most likely due to a large amount of maternally loaded mRNA in the zygote that is utilized by the embryo. Alternatively, the promoter itself is 'leaky', meaning there is transcription of the gene even where we wouldn't predict any to be. This could explain why in the germline (P) lineage analysis there is a slight increase in the amount of fluorescent histone incorporated into the chromatin at metaphase in the later cells, and this is not seen in the other somatic (AB and E) lineages (Figure 1D-E and Figure 2A). This promoter could also explain why we see an 'overloading' of fluorescent histone into the nucleus, which then dissipates into the cytoplasm upon NEBD. These 'extra' histones are not deleterious to mitotic fidelity as we see no impact on hatch/growth rate or incidence of males in this strain of worms (data not shown)[30]. We also note that even though the levels of the histone are different between the different lineages; although, each lineage is normalized to itself, allowing us to correct for these differences. Despite these potential limitations to our system, we find that the dynamics and characteristics of H2B in this system behave as we would predict them to.

We confirmed that throughout all of the cell cycles analyzed in early development, there was the expected rise of nuclear levels within each cycle cell from beginning to end. This rise in nuclear levels of canonical histones is always associated with S-Phase, when histones are transcribed, translated, and imported into the nucleus for incorporation into newly replicated chromatin. In *C. elegans* we see the rise occurring in the very early part of each cell cycle, usually occurring within the first ten minutes of the beginning of each cell cycle. Given that all of the early cells in the embryo are not known to have any GAP phases, instead, DNA replication takes the entirety of the interphase cell cycle, it makes sense that we would see histones begin to accumulated in the nucleus so quickly after mitosis terminates.

We also find that the data alignment application results in smoother curves (when n is high enough) that are potentially more biologically realistic than the data aligned strictly by their time-points. However, the somatic cell cycles, which were composed of smaller datasets, had averages that seemed more susceptible to outliers, especially near the beginning and ends of the timelapses. This is because as the program explores all the possible ways to shift the timepoints of the datasets, it might reduce the standard deviation around the mean, but may cause points at the beginning or end of the timelapses to stick out in the average.

FRAP analysis showed that using unbleached embryos as a control group are sufficient to calculate turnover in our system. We find that although there is variation in the quantity of fluorescent histones measured per cell, overall the average in the controls is double the starting value, which is consistent with our understanding of canonical histone incorporation. Unless there is a significant change to the genome size, there will not be a change in the quantity of histones that are needed to be reconstituted each cell cycle. Because the controls were all imaged identically, they were averaged together to create a Final (Control) value. Because each photobleached embryo was bleached to a different percent of its original signal (due to movement of the nucleus during the bleaching process) each time lapse was one Final (FRAP) value. From these calculations and the fact that our average bleach efficiency of the original signal was around 70%, we found that all of the turnovers fell within that error margin. So, although there may be some amount of turnover, it’s not obviously apparent exactly how much that is, although we definitely do not have a complete recovery of signal as would be expected for a turnover of 100%. The stability of the histones means that the short and relatively unchanging recovery rates are a reflection of how long the turnover takes from the beginning after the cell cycle starts, and the time it takes to completely turnover does lengthen slightly with the lengthening of the cell cycle.

With the exception of a few outliers, there really isn't any strong correlation in any of the plots, suggesting that turnover is quite stable during the first few cell divisions and between lineages. We suspect that the histones are relatively stable in these early cell divisions because there is little to no detectable transcription occurring during any of the cell cycles that we performed FRAP experiments on. We predict, that if we were able to perform the FRAP experiments in the much longer somatic lineages (P-lineage has no transcription[31]) that we might see some measurable turnover of the histones.

Overall, we find that utilizing an extremely well-studied protein in a very well understood model system has been ideal for creating an embryonic experimental system where we can combine techniques from a variety of well-established cell cycle analysis pipelines for exploring protein dynamics and turnover. The analysis pipeline we have described here can be applied to any fluorescently labeled protein with a reasonable signal to noise ratio. It can be utilized in systems were temporal and spatial resolution are not cutting edge, or in systems where traditional synchronization and bulk biochemical analyses have been unable to be performed before. Although there is a larger amount of variation within the data than is usually appreciated in these types of experiments, information about the biology of these systems can still be produced, interpreted and appreciated despite their 'setbacks'.

## Materials and Methods

### C. elegans strains

Worms were cultured and imaged at 20°$^{c}$ on OP50 seeded agar plates as described in Riddle *et al* [32]. All worms used for imaging were from non-starved populations. The *C. elegans* strains used here (OD421 & OD145) were a generous gift from the Desai and Oegema labs. OD421 is a triple mutant composed of a composition of the following strains: CeCENP-A/*hcp-3* deletion allele *ok1892*, GFP-CeCENP-A (OD347), and *pie-1p*:mCherry-histone H2B (OD56)[33].

### Microscopy

#### Cell Identification.

Cell identification was performed through manual lineage tracing from at least the 4-cell stage in the early *C. elegans* embryos. The late P-lineage identification was aided by the extra fluorescence in the red channel driven by the pie-1 promoter driving mCherry::H2B. Cellular morphology, movement, and cell cycle duration was used to confirm the identification of cells.

**Sample preparation and imaging of embryos.**

(Our protocol is adapted from Monica Driscoll's protocol on Wormbook. Embryos were dissected out of non-starved, gravid adult *C. elegans* into M9 on No.1.5 22mm$^2$ coverslips and mounted onto 2% (w/v) agar pads on a standard microscopy slide, before being sealed with VALAP (1:1:1 lanolin, petroleum jelly, and parafilm wax). 2% agar pads were used to gently compress embryos without damaging them. Imaging was performed on a Nikon A1R microscope body with a 60X 1.27 NA Nikon Water Immersion Objective with a GaASP PMT detector (Nikon) using NIS-elements. Imaging was done using excitation of mCherry fluorophores using 561nm lasers respectively. Z-stacks contained between 20-30 slices (depending on how embryo was oriented), and all slices were 1µm apart. Z-stacks were collected every 2 minutes for approximately 1-3 hours for early embryo timelapses, and for the entire duration of each cell cycle for FRAP analysis.

**Image Analysis.**

Images collected using NIS-Elements were imported for analysis in ImageJ/FIJI. All Z-stacks were transformed into individual Max-Projections throughout the entire embryo before drawing regions of interest (ROIs) and taking measurements. If a Max-Intensity-Projection throughout the entire embryo was not appropriate for measuring a single nucleus in a crowded embryo, individual Max-Projections were generated for each time point. For every timepoint, a ROI was drawn around the entire nucleus of interest, and two or three ROIs of equal size were collected from the cytoplasm. Collection of measurements were expedited using custom macros. For our analysis we used the values generated in ImageJ/FIJI labeled RawIntDen, which is the sum of all gray values in an ROI. These 'background' ROIs were averaged, area corrected, bleach corrected (for timelapses, not FRAP analysis), and their Raw-Integrated-Density (RawIntDen) values were subtracted from the nuclei RawIntDen value to create the 'Raw (Background Corrected) Nuclear Intensity. Example image in Supplemental Figure 1.

**Figure Legends**

**Graphical Abstract. Schematic of analysis pipelines of embryonic timelapse data from raw image data to graphs.**

Novel embryo analysis pipeline to: take raw image data (3D stacks taken over time), measure nuclear signal, a primary normalization and arrangement, graphing and interpreting the data,

performing a secondary arrangement, and creating a final graph. Our FRAP Analysis pipeline involves using both bleached and control embryos imaged under identical conditions, normalized and arranged before using the calculated values to quantify turnover of a fluorescently labeled protein.

**Figure 1. Embryo analysis pipeline involving normalization, organization, and secondary analysis facilitate quantification of canonical histone behavior in C. elegans embryos.**
(A) Representative image of a timelapse image of the 1-cell through ~100-cell embryo. The P-lineage is indicated and representative first and lapse timepoints for each cell cycle are shown. Developmental time indicated in minutes post 2-cell stage. (B) Representative image of multiple, asynchronous embryos imaged simultaneously. (C) Schematic of data normalization and primary arrangements. For lineage arrangements, all cell cycles are aligned to the last timepoint regardless of cell cycle length (~metaphase). All timelapses must contain a shared cell cycle event (*), the nuclear value at this point was set to 1 within each timelapse. Resulting primary $^{1}$averages can be then be calculated. (D-E) Timepoints are 2-minutes apart. Grey column represents approximate time of NEBD. Small triangle indicates alignment point. Experimental $^{1}$averages and standard deviations are plotted. (D) P-lineage experimental data plotted. (*) is the first timepoint of P3. (E) E-lineage (left) and AB-lineage (right) experimental data plotted. (*) is first timepoint of E and ABa respectively. (F) Using the calculated $^{1}$average and the same data sets, the data is run through our custom MATLAB macro to generated new timestamps to decrease the standard deviation around the $^{1}$average, resulting in a new $^{2}$average generated as a histogram with 1 timepoint (2-minute) bins. (G-H) Experimental $^{2}$averages and standard deviations are plotted. (G) P-lineage experimental data plotted. (H) E-lineage (left) and AB-lineage (right) experimental data plotted.

**Table 1. List of calculated values for quantifying nuclear accumulation of H2B.**
(1) Cell cycle analyzed. (2) Rise in nuclear signal measured for each cell cycle of the three lineages quantified in minutes. (3) Relative levels of mCherry::H2B from $^{1}$lineage analysis (Figure 1) (left), then normalized to the cell value from the 4-cell embryo (P2/EMS/ABa) (right). (4) Calculated number of histones with 1.00 = $9.9 \bullet 10^{5}$ histones. (5) Values in Column 3 and multiplied by values in Column 4. (6) Number of timelapses used to generate the calculated accumulation.

**Figure 2. Histone nuclear import rates scale inversely to cell cycle length.**

(A) A germline-specific-promoter drives increased fluorescently labeled histone in the P-lineage, whereas the amount of fluorescently labeled histone incorporated into chromatin is stable through the 4-cell stage and decreases starting around the 8-cell stage of the somatic lineages. Identical data to Figure 1D-E each normalized internally to their own lineages (*). (B) Plotted calculations of H2B nuclear accumulation rates throughout development. Boxes represent standard deviation of the mean for both cell cycle length (horizontal) and nuclear accumulation rate (vertical). Solid line is a best fit one phase exponential decay curve, equation shown.

**Figure 3. Protein stability and turnover dynamics can be quantified using population controls to reveal stable chromatin incorporation.**

(A) Max-projections of representative images of Control (top) and Bleached (bottom) embryos. Images are scaled and aligned identically with first and last timeframes of specific cells (P1) indicated. (B) Example of where in each timelapse data is normalized and collected from to calculate turnover. (C) Experimental values of Final Values for Control and Bleached conditions for 5 different cells. (D) Calculated turnover values for 5 cells from early embryo. (E-G) Linear regression lines for somatic cells (pink), germline cells(yellow), and both (black) with 95% confidence interval bands. (E) Turnover values plotted against cell cycle length. (F) Calculated values of Cell Cycle length, $t_{1/2}$, and Recovery Rate. (G) Cell cycle length plotted against calculated recovery rate. (H) Cell cycle length plotted against calculated $t_{1/2}$.

**Supplemental 1. Representative image of manually collecting ROIs for measurement/quantification.**

$Nuclear_{ROI}$s refer to drawing an ROI around a circular nucleus (pre-NEBD) (left) or chromatin (post-NEBD) (right). $Background_{ROI}$s refer to drawing an ROI anywhere in the cytoplasm of the cell/embryo being analyzed.

**Acknowledgements**

We would like to give a huge thanks to all the members of both Paul Maddox and Amy Maddox's labs especially to Vincent Boudreau and Jake Sellinger who read this manuscript and helped develop the MATLAB macro used respectively. Special thanks to Kerry Bloom for his mentorship and guidance as well as reading this manuscript. We would also like to thank the Oegema/Desai labs for the worm strain used in this publication. This work was funded by the National Science Foundation CAREER Award 1652512.

## Author Contributions

*Conceived and designed the experiments:* Lydia Smith and Paul Maddox. *Performed the experiments:* Lydia Smith. *Analyzed the data:* Lydia Smith. *Wrote the paper:* Lydia Smith and Paul Maddox.

## Abbreviations Used

AU: Arbitrary Units
Ave: Average
FRAP: Fluorescence Recovery After Photobleaching
H2B: Histone 2B
Max-Projection: Maximum-Intensity-Projection
MGV: Mean Grey Value
NEBD: Nuclear Envelope BreakDown
RID: RawIntDen: Raw Integrated Density
ROI: Region of Interest

**Bibliography**


[1] D. R. Foltz, L. E. T. Jansen, A. O. Bailey, J. R. Yates, E. A. Bassett, S. Wood, B. E. Black, and D. W. Cleveland, “Centromere-specific assembly of CENP-a nucleosomes is mediated by HJURP.,” *Cell*, vol. 137, no. 3, pp. 472–84, May 2009.

[2] M. A. Juanes, “Methods of Synchronization of Yeast Cells for the Analysis of Cell Cycle Progression,” in *Methods in molecular biology (Clifton, N.J.)*, vol. 1505, 2017, pp. 19–34.

[3] A. L. Mattheyses, S. M. Simon, and J. Z. Rappoport, “Imaging with total internal reflection fluorescence microscopy for the cell biologist.,” *J. Cell Sci.*, vol. 123, no. Pt 21, pp. 3621–8, Nov. 2010.

[4] L. E. T. Jansen, B. E. Black, D. R. Foltz, and D. W. Cleveland, “Propagation of centromeric chromatin requires exit from mitosis.,” *J. Cell Biol.*, vol. 176, no. 6, pp. 795–805, Mar. 2007.

[5] V. Roukos, G. Pegoraro, T. C. Voss, and T. Misteli, “Cell cycle staging of individual cells by fluorescence microscopy,” *Nat. Protoc.*, vol. 10, no. 2, pp. 334–348, Jan. 2015.

[6] M. F. Z. Wang, M. V Hunter, G. Wang, C. McFaul, C. M. Yip, and R. Fernandez-Gonzalez, “Automated cell tracking identifies mechanically oriented cell divisions duringDrosophilaaxis elongation.,” *Development*, vol. 144, no. 7, pp. 1350–1361, Apr. 2017.

[7] A. Philpott and P. R. Yew, “The Xenopus cell cycle: an overview.,” *Methods Mol. Biol.*, vol. 296, pp. 95–112, 2005.

[8] E. T. Kipreos, “C. elegans cell cycles: invariance and stem cell divisions,” *Nat. Rev. Mol. Cell Biol.*, vol. 6, no. 10, pp. 766–776, Oct. 2005.

[9] W. Huang, F. Arai, and T. Kawahara, “Egg-in-Cube: Design and Fabrication of a Novel Artificial Eggshell with Functionalized Surface,” *PLoS One*, vol. 10, no. 3, p. e0118624, Mar. 2015.

[10] S. Ishiura, Ed., “11.5 ECM | Introduction to Life Science | University of Tokyo,” *a comprehensive approach to Life Science*, 2010. [Online]. Available: http://csls-text3.c.u-tokyo.ac.jp/active/11_05.html. [Accessed: 30-Mar-2018].

[11] J. E. E. Sulston, E. Schierenberg, J. G. G. White, and J. N. N. Thomson, “The embryonic cell lineage of the nematode Caenorhabditis elegans.,” *Dev. Biol.*, vol. 100, no. 1, pp. 64–119, Nov. 1983.

[12] L. Byerly, R. C. Cassada, and R. L. Russell, “The Life Cycle of the Nematode Caenorhabditis elegans,” *Dev. Biol.*, vol. 33, no. 1, pp. 23–33, Jul. 1976.

[13] A. Miyawaki, “Green Fluorescent Protein-like Proteins in Reef Anthozoa Animals,” *Cell*

*Struct. Funct.*, vol. 27, no. 5, pp. 343–347, 2002.

[14] T. J. Boyle, Z. Bao, J. I. Murray, C. L. Araya, and R. H. Waterston, “AceTree: a tool for visual analysis of Caenorhabditis elegans embryogenesis.,” *BMC Bioinformatics*, vol. 7, p. 275, Jun. 2006.

[15] P. Xenopoulos, S. Nowotschin, and A.-K. Hadjantonakis, “Chapter eighteen – Live Imaging Fluorescent Proteins in Early Mouse Embryos,” in *Methods in Enzymology*, vol. 506, 2012, pp. 361–389.

[16] P. E. Young, T. C. Pesacreta, and D. P. Kiehart, “Dynamic changes in the distribution of cytoplasmic myosin during Drosophila embryogenesis.,” *Development*, vol. 111, no. 1, pp. 1–14, Jan. 1991.

[17] R. Schnabel, M. Bischoff, A. Hintze, A.-K. Schulz, A. Hejnol, H. Meinhardt, and H. Hutter, “Global cell sorting in the C. elegans embryo defines a new mechanism for pattern formation,” *Dev. Biol.*, vol. 294, no. 2, pp. 418–431, Jun. 2006.

[18] J. C. Waters, “Accuracy and precision in quantitative fluorescence microscopy.,” *J. Cell Biol.*, vol. 185, no. 7, pp. 1135–48, Jun. 2009.

[19] S. Gookin, M. Min, H. Phadke, M. Chung, J. Moser, I. Miller, D. Carter, and S. L. Spencer, “A map of protein dynamics during cell-cycle progression and cell-cycle exit,” *PLOS Biol.*, vol. 15, no. 9, p. e2003268, Sep. 2017.

[20] J. Berro and T. D. Pollard, “Local and global analysis of endocytic patch dynamics in fission yeast using a new "temporal superresolution" realignment method.,” *Mol. Biol. Cell*, vol. 25, no. 22, pp. 3501–14, Nov. 2014.

[21] L. W. Hillier, A. Coulson, J. I. Murray, Z. Bao, J. E. Sulston, and R. H. Waterston, “Genomics in C. elegans: so many genes, such a little worm.,” *Genome Res.*, vol. 15, no. 12, pp. 1651–60, Dec. 2005.

[22] H. J. Szerlong and J. C. Hansen, “Nucleosome distribution and linker DNA: connecting nuclear function to dynamic chromatin structure.,” *Biochem. Cell Biol.*, vol. 89, no. 1, pp. 24–34, Feb. 2011.

[23] P. S. Maddox, K. S. Bloom, and E. D. Salmon, “The polarity and dynamics of microtubule assembly in the budding yeast Saccharomyces cerevisiae,” *Nat. Cell Biol.*, vol. 2, no. 1, pp. 36–41, Jan. 2000.

[24] M. L. Kireeva, W. Walter, V. Tchernajenko, V. Bondarenko, M. Kashlev, and V. M. Studitsky, “Nucleosome Remodeling Induced by RNA Polymerase II: Loss of the H2A/H2B Dimer during Transcription,” *Mol. Cell*, vol. 9, no. 3, pp. 541–552, Mar. 2002.

[25] O. I. Kulaeva, D. A. Gaykalova, and V. M. Studitsky, “Transcription through chromatin by

RNA polymerase II: Histone displacement and exchange," *Mutat. Res. Mol. Mech. Mutagen.*, vol. 618, no. 1–2, pp. 116–129, May 2007.

[26] S. C. Tintori, E. Osborne Nishimura, P. Golden, J. D. Lieb, and B. Goldstein, "A Transcriptional Lineage of the Early C. elegans Embryo," *Dev. Cell*, vol. 38, no. 4, pp. 430–444, Aug. 2016.

[27] H. S. Malik and S. Henikoff, "Phylogenomics of the nucleosome," *Nat. Struct. Mol. Biol.*, vol. 10, no. 11, pp. 882–891, Nov. 2003.

[28] M. A. Osley, "The Regulation of Histone Synthesis in the Cell Cycle," *Annu. Rev. Biochem.*, vol. 60, no. 1, pp. 827–861, Jun. 1991.

[29] M. Fukuyama, A. E. Rougvie, and J. H. Rothman, "C. elegans DAF-18/PTEN mediates nutrient-dependent arrest of cell cycle and growth in the germline.," *Curr. Biol.*, vol. 16, no. 8, pp. 773–9, Apr. 2006.

[30] J. Hodgkin, H. R. Horvitz, and S. Brenner, "Nondisjunction Mutants of the Nematode CAENORHABDITIS ELEGANS.," *Genetics*, vol. 91, no. 1, pp. 67–94, Jan. 1979.

[31] D. Ghosh and G. Seydoux, "Inhibition of Transcription by the Caenorhabditis elegans Germline Protein PIE-1: Genetic Evidence for Distinct Mechanisms Targeting Initiation and Elongation," *Genetics*, vol. 178, no. 1, pp. 235–243, Jan. 2008.

[32] D. L. Riddle, T. Blumenthal, B. J. Meyer, and J. R. Priess, *C. elegans II*. Cold Spring Harbor Laboratory Press, 1997.

[33] R. Gassmann, A. Rechtsteiner, K. W. Yuen, A. Muroyama, T. Egelhofer, L. Gaydos, F. Barron, P. Maddox, A. Essex, J. Monen, S. Ercan, J. D. Lieb, K. Oegema, S. Strome, and A. Desai, "An inverse relationship to germline transcription defines centromeric chromatin in C. elegans.," *Nature*, vol. 484, no. 7395, pp. 534–7, Apr. 2012.

# Graphical Abstract

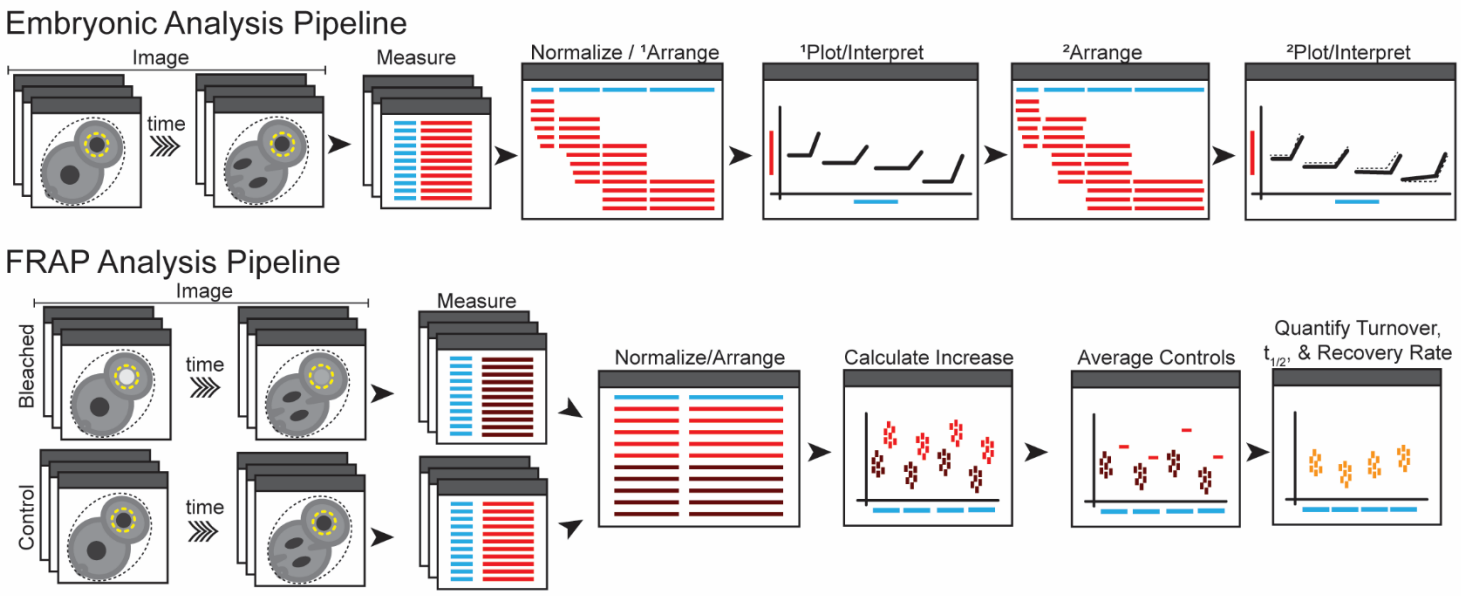

# Figure 1

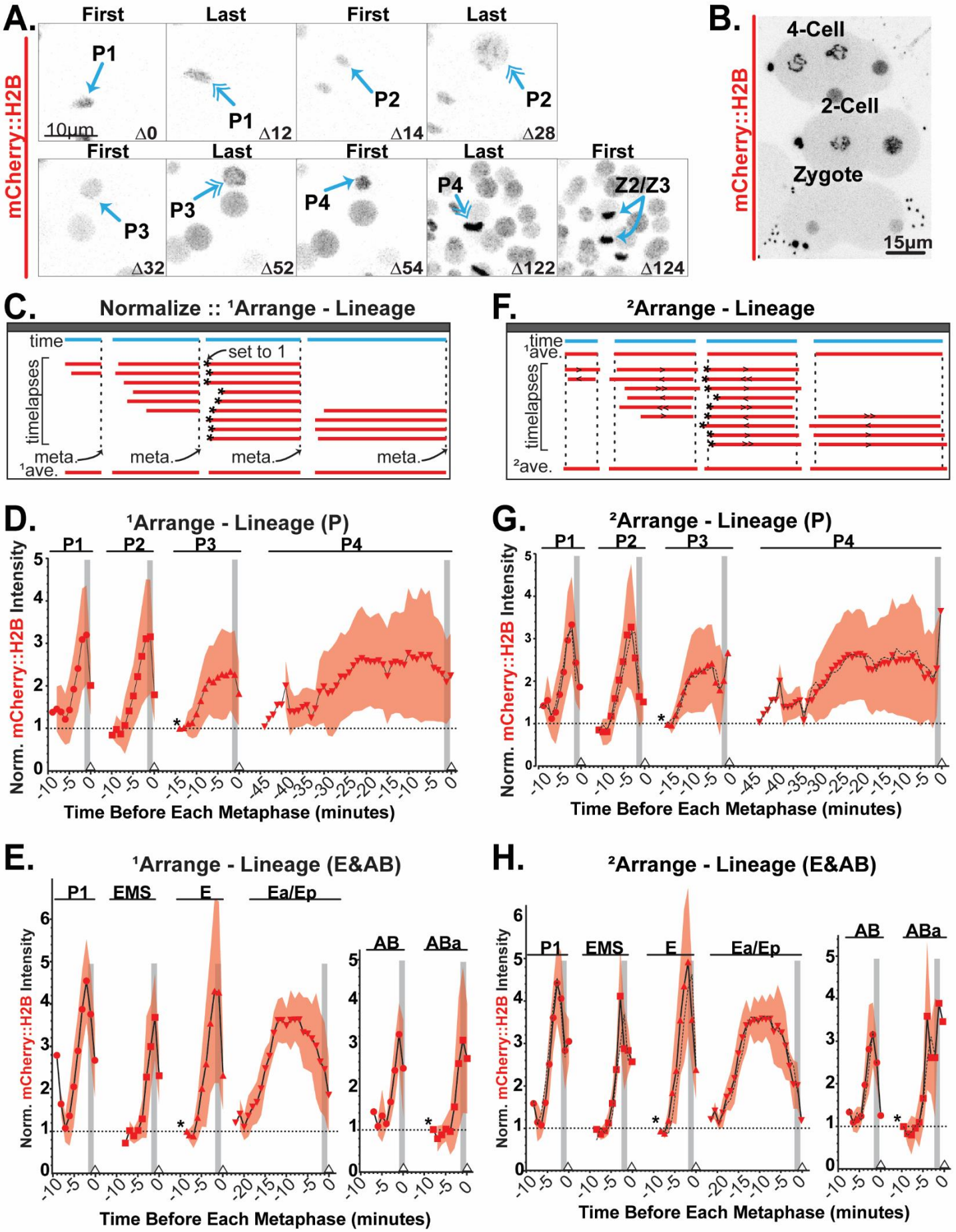
A.
First
Last
First
Last
mCherry::H2B
P1
P1
P2
P2
10µm
Δ0
Δ12
Δ14
Δ28
First
Last
First
Last
First
P3
P3
P4
P4
Z2/Z3
Δ32
Δ52
Δ54
Δ122
Δ124
B.
4-Cell
2-Cell
Zygote
mCherry::H2B
15µm
C.
Normalize :: ¹Arrange - Lineage
time
set to 1
timelapses
meta.
¹ave.
F.
²Arrange - Lineage
time
¹ave.
timelapses
²ave.
D.
¹Arrange - Lineage (P)
P1
P2
P3
P4
Norm. mCherry::H2B Intensity
Time Before Each Metaphase (minutes)
G.
²Arrange - Lineage (P)
E.
¹Arrange - Lineage (E&AB)
P1
EMS
E
Ea/Ep
AB
ABa
H.
²Arrange - Lineage (E&AB)

# Table 1

| [1]Cell | [2]Import Duration | [3]Relative Metaphase Levels (versus 4-cell) | | [4]Histone Added | [5]Nuclear Accumulation (histones/min) | [6]n |
|---|---|---|---|---|---|---|
| P1 | 12.3 (± 2.13) | 2.03 | 1.09 | $1.08 \cdot 10^6$ | $7.36 (\pm 2.27) \cdot 10^4$ | 10 |
| P2 | 12.9 (± 2.56) | 1.86 | 1.00 | $0.99 \cdot 10^6$ | $6.08 (\pm 2.52 \cdot 10^4$ | 18 |
| P3 | 12.6 (± 3.54) | 1.83 | 0.98 | $0.97 \cdot 10^6$ | $4.00 (\pm 1.59) \cdot 10^4$ | 20 |
| P4 | 15.6 (± 5.17) | 2.16 | 1.16 | $1.15 \cdot 10^6$ | $1.79 (\pm 0.76) \cdot 10^4$ | 6 |
| P1 | 11 (± 2.58) | 2.68 | 1.03 | $1.02 \cdot 10^6$ | $4.98 (\pm 2.34) \cdot 10^4$ | 4 |
| EMS | 8.8 (± 2.52) | 2.60 | 1.00 | $0.99 \cdot 10^6$ | $6.19 (\pm 0.97) \cdot 10^4$ | 10 |
| E | 11.1 (± 3.18) | 2.50 | 0.96 | $0.95 \cdot 10^6$ | $5.60 (\pm 1.88) \cdot 10^4$ | 9 |
| Ea/Ep | 10.6 (± 2.73) | 1.86 | 0.72 | $0.71 \cdot 10^6$ | $1.75 (\pm 0.80) \cdot 10^4$ | 6 |
| AB | 6.8 (± 1.51) | 2.45 | 0.91 | $0.91 \cdot 10^6$ | $7.94 (\pm 2.85) \cdot 10^4$ | 7 |
| ABa | 7.7 (± 1.56) | 2.68 | 1.00 | $0.99 \cdot 10^6$ | $9.61 (\pm 6.22) \cdot 10^4$ | 9 |

# Figure 2

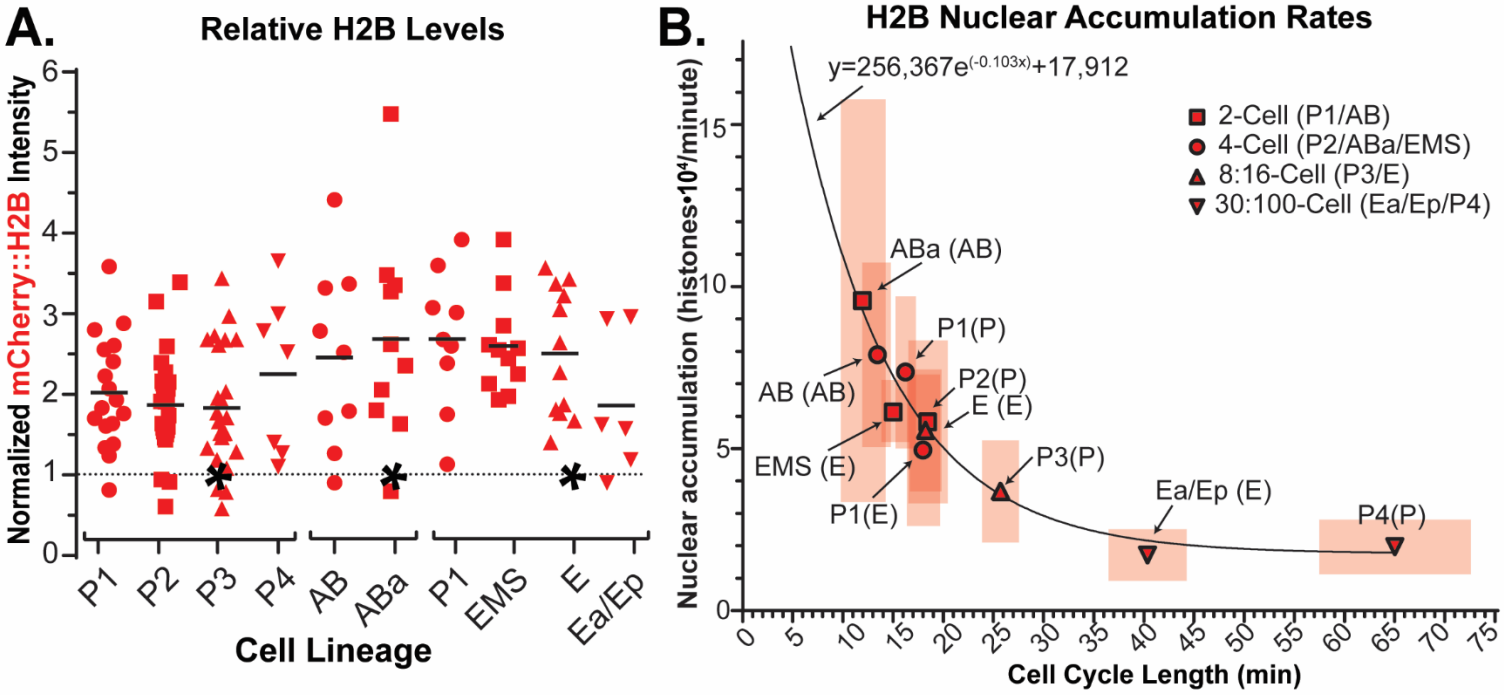
A.
Relative H2B Levels
Normalized mCherry::H2B Intensity
0
1
2
3
4
5
6
P1
P2
P3
P4
AB
ABa
P1
EMS
E
Ea/Ep
Cell Lineage
B.
H2B Nuclear Accumulation Rates
y=256,367e(-0.103x)+17,912
2-Cell (P1/AB)
4-Cell (P2/ABa/EMS)
8:16-Cell (P3/E)
30:100-Cell (Ea/Ep/P4)
ABa (AB)
P1(P)
AB (AB)
P2(P)
E (E)
EMS (E)
P3(P)
P1(E)
Ea/Ep (E)
P4(P)
Nuclear accumulation (histones•10⁴/minute)
0
5
10
15
0
5
10
15
20
25
30
35
40
45
50
55
60
65
70
75
Cell Cycle Length (min)

# Figure 3

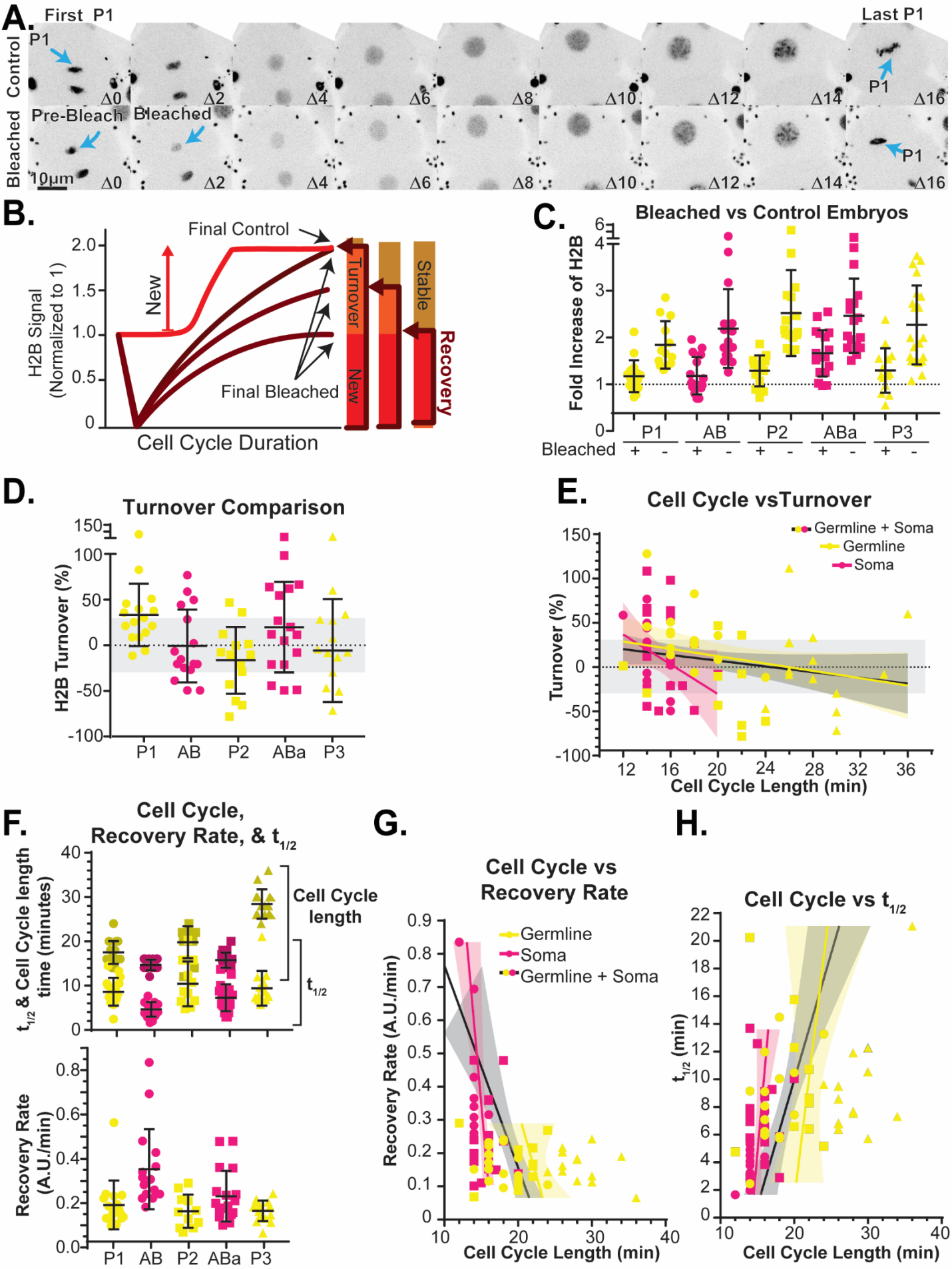
A.
First P1
Last P1
Control
P1
Δ0
Δ2
Δ4
Δ6
Δ8
Δ10
Δ12
Δ14
Δ16
Bleached
Pre-Bleach
Bleached
10µm
B.
Final Control
New
Final Bleached
H2B Signal (Normalized to 1)
Cell Cycle Duration
Turnover
Stable
Recovery
C.
Bleached vs Control Embryos
Fold Increase of H2B
P1
AB
P2
ABa
P3
Bleached
D.
Turnover Comparison
H2B Turnover (%)
E.
Cell Cycle vsTurnover
Germline + Soma
Germline
Soma
Turnover (%)
Cell Cycle Length (min)
F.
Cell Cycle, Recovery Rate, & t1/2
t1/2 & Cell Cycle length time (minutes)
Cell Cycle length
t1/2
Recovery Rate (A.U./min)
G.
Cell Cycle vs Recovery Rate
Germline
Soma
Germline + Soma
Recovery Rate (A.U./min)
Cell Cycle Length (min)
H.
Cell Cycle vs t1/2
t1/2 (min)
Cell Cycle Length (min)
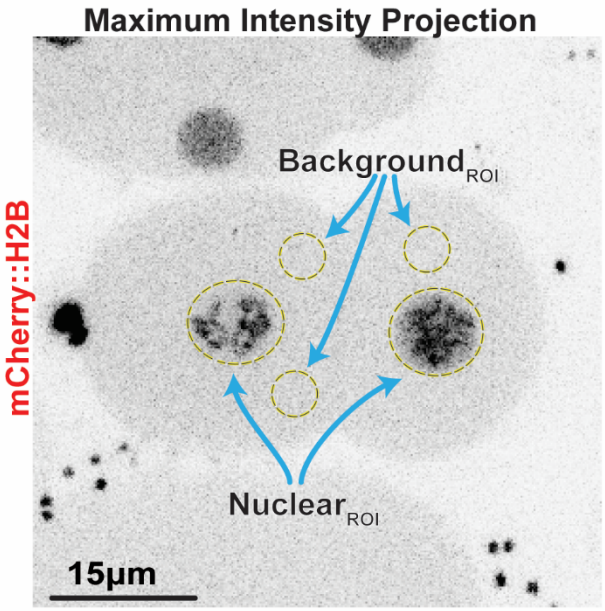
# Supplemental Figure 1